ARTICLE

Dual Synergistic Modulation of Photo-Induced Electron Transfer Processes Between Molecules and Gold Nanopillars for Ultrasensitive Plasmon-Enhanced Raman Scattering

Received 00th January 20xx,
Accepted 00th January 20xx

DOI: 10.1039/x0xx00000x

Iris B. Ansah,[a,b,†] Daniel Aranda,[c,†] Ho S. Jung,[a] Sung-Gyu Park,[a] Mijeong Kang,[d,*] Juan C. Otero,[e,*] and Dong-Ho Kim[a,b,*]

This work presents a synergistic approach to boost plasmon- or surface-enhanced Raman scattering (SERS) by combining molecular and electrical modulators that fine-tune the electronic structure of metal–molecule interfaces, especially the charge transfer (CT) states, allowing molecular resonances. Paraquat (PQ^{2+}) was interfaced with nanopillar SERS substrates whose surface excess of charge was modulated by intercalating anionic Au complexes ($AuCl_4^-$, $Au(CN)_2^-$) as well as by applying external electric potentials. Such concurrent dual modulation tuned the energy of the CT states of the substrate−anion−PQ^{2+} triads in resonance with the excitation laser, resulting in a large enhancement of the PQ^{2+} SERS bands. The results point to a novel coherent through-bond CT contribution of SERS, analogous to the superexchange mechanism for electron transfer in donor−bridge−acceptor systems. The large amplification enables high sensitivity for detecting PQ^{2+} and ultimately enables the on-site detection of PQ^{2+} in unprocessed real samples (coffee drink). This study account for new physicochemical variables affecting electron transfer processes in nanostructured metal-molecule interfaces and provides a path for further exploring chemical strategies for greater Raman enhancement and for developing ultrasensitive Raman platforms.

Introduction

Raman scattering has been used in fundamental research on the physical chemistry of molecules and in practical analytical applications for molecular detection.[1] Enhancement of Raman scattering by localized surface plasmons, termed plasmon- or surface-enhanced Raman scattering (SERS), has greatly expanded the use of Raman spectroscopy as a sensitive analytical technique over the past four decades, driven by the explosive development of new nanoplasmonic substrates.[2-5] In addition to this material-wise contribution, modulating the complex electronic structure of metal–molecule interfaces can intensify the light–molecule interaction and thereby further enhance the SERS signal, which is known as the chemical enhancement mechanism of SERS.

The most important chemical contribution to SERS is based on resonance Raman scattering involving new electron or charge transfer (CT) states[6-8] of the supramolecular system formed by the nanostructured metallic substrate and the adsorbed molecule. In this resonant process, an electron is photoexcited to a CT state of the complex, resulting in an enhancement of the Raman signal, where specific molecular vibrations are selectively intensified. The CT-resonant condition is fulfilled when the energy of the incident laser matches the energy gap between the ground and CT excited states of the surface complex.[9] Given the limited number of standard lasers used in Raman excitation, an alternative strategy to achieve the CT-resonance Raman condition is to modulate the electronic structure of the complex by applying external electric potentials (E_V).[10-13] Electrode potentials control the surface excess of charge of the metallic substrate, and this excess of charge is responsible for modifying the metal–molecule bond strength and especially the energies of the CT excited states.[13-14]

We herein propose a novel approach to further enhance SERS signals by fine-tuning the resonant CT processes by manipulating the interplay between molecular and electrical modulators. In addition to electric potentials (the “electrical” modulator), we introduce an enhancer molecule (the “molecular” modulator) that forms a supramolecular complex with the Raman-active molecule and brings the electronic structure of the triad (metal surface–enhancer–Raman molecule) into resonance with the laser light. This study reports the discovery of the complementary combination of proper chemical species (a molecular modulator) combined with the

[a] Nano-Bio Convergence Department, Korea Institute of Materials Science (KIMS), Changwon, Gyeongnam 51508, Republic of Korea
[b] Advanced Materials Engineering Division, University of Science and Technology (UST), Daejeon 34113, Republic of Korea
[c] Istituto di Chimica dei Composti Organometallici, Consiglio Nazionale delle Ricerche (ICCOM-CNR), 56124, Pisa, Italy
[d] Department of Cogno-Mechatronics Engineering, Pusan National University (PNU), Busan 46241, Republic of Korea
[e] Universidad de Málaga, Andalucía Tech, Facultad de Ciencias, Departamento de Química Física, 29071-Málaga, Spain
† These authors contributed equally.
* Corresponding authors
Electronic Supplementary Information (ESI) available: [Theoretical methods (computational details), Figures S1-S10.]. See DOI: 10.1039/x0xx00000x

tuning effect of the applied voltage (an electrical modulator) to attain huge SERS enhancement of selected molecules. The proposed approach enables amplification of the SERS response of molecules with a low affinity to metal substrates (e.g., positively charged species) and further improves the capabilities of SERS as an ultrasensitive sensor platform. Finally, this work opens also new insights on the mechanism of electron transfer processes in nanostructured interfaces which could help for improving the performance of molecular electronic devices.

Results and discussion

The studied SERS-active molecule was paraquat (PQ^{2+}, 1,1′-dimethyl-4,4-bipyridinium or methyl viologen), which has two aromatic rings, each containing a quaternary nitrogen and providing two positive charges to the system. Molecular cations such as PQ^{2+} exhibit poor affinity to metal substrates because they are electron-deficient; consequently, SERS spectra of these cations are usually recorded by intercalating simple anionic species such as halogen ions.[15] The normal Raman spectrum of a saturated solution of PQ^{2+} in deionized water (Figure 1a) shows strong bands at 839, 1185, 1279, and 1639 cm^{-1}, which are assigned to ring-breathing, N–CH_3 stretching, C–H bending, and ring-stretching fundamentals, respectively, according to B3LYP/LanL2DZ calculations (Figures S1 and S2). Au nanopillars (see Figure S3 and the fabrication details in Methods) were used as a SERS substrate, and the corresponding spectrum of an aqueous solution of $PQCl_2$ at a low concentration (5 µM) in the presence of an excess of chloride ions (0.1 M NaCl, added to enable electrochemical experiments; see details in Methods) exhibited weak PQ^{2+} bands (Figure 1a). SERS spectra of this sample showed a rather weak enhancement when the spectra were recorded under applied electric potentials (SERS signals measured under potential application are called EC-SERS hereafter) ranging from −0.5 V to +0.5 V *vs* Ag/AgCl (3 M NaCl) reference electrode (Figure 1b).

Cl^- and CN^- ions are strongly polarizing[16] and are known to form electrostatic complexes with PQ^{2+}. In addition, anionic

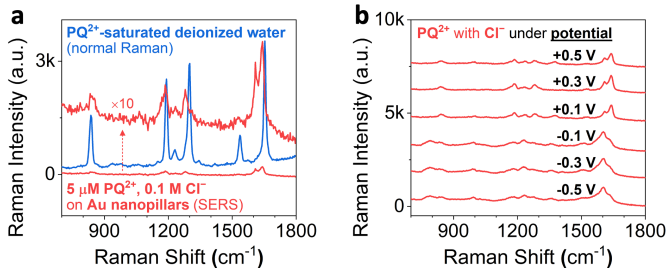

Figure 1. (a) Normal Raman spectrum of a saturated solution of PQ^{2+} in deionized water (blue) and SERS spectrum of 5 µM PQ^{2+} and 0.1 M Cl^- aqueous solution on Au nanopillars (red). (b) Effect of applied electric potentials on the SERS spectrum of 5 µM PQ^{2+} solutions on Au nanopillars in the presence of 0.1 M NaCl. Laser line: 785 nm.

systems can interact with electron-deficient aromatic systems such as PQ^{2+} via anion–π interaction,[17-21] which has recently gained recognition as an unconventional intermolecular interaction in supramolecular architectures. Cl^- and CN^- were initially examined as enhancers of the SERS of PQ^{2+} but proved ineffective, as shown in Figure 2a, where the spectra were recorded at the respective open-circuit potentials (OCPs). The overall and relative SERS intensities recorded without (in deionized water) and with additional added Cl^- (1 mM) or CN^- (1 mM) anions in the presence of excess Cl^- (0.1 M) are almost identical, and the samples exhibit similar OCP values. These results indicate that the Cl^- ions of the 5 µM $PQCl_2$ sample should be sufficient for trapping PQ^{2+} cations on the substrate and that neither excess Cl^- (0.1 M or 1 mM) nor CN^- (1 mM) play a substantial role in enhancing these SERS.

Recent theoretical studies have demonstrated the feasibility of complex anions containing coinage metals to form supramolecular structures with electron-deficient aromatic rings.[21-23] To investigate the effect of these anionic complexes on the SERS of PQ^{2+}, we added tetrachloroaurate(III) ($AuCl_4^-$, 1 mM) and dicyanoaurate(I) ($Au(CN)_2^-$, 1 mM) to PQ^{2+} solution (5 µM), whose molecular structures are shown in Figure 2c. Both complexes strongly enhance the PQ^{2+} SERS signal and, interestingly, do so in a differentiated manner. This enhancement is clearly observed by Au nanopillars (Figure 2a), but not by flat Au substrates (Figure 2b), what confirms the requirement of using plasmonic nanostructures in order to get strong SERS effect. As shown in Figure 2a, the SERS spectrum recorded when $AuCl_4^-$ was present is dominated by the three PQ^{2+} bands with lower or medium wavenumbers at 839, 1185, and 1279 cm^{-1}, which are enhanced 20, 25, and 12 times, respectively. They are also intensified in the SERS with $Au(CN)_2^-$; however, in this case, the highest-wavenumber band at 1639 cm^{-1} shows the largest selective enhancement, whereas it was very weak in the spectrum with $AuCl_4^-$. This band is characteristic of the ring-stretching vibration of benzene-like molecules containing six-membered aromatic rings. It is assigned to the 8a normal mode and corresponds, in this case, to the symmetric combination (8a+8a') of the stretching of both rings of PQ^{2+} under the C_2 point group (Figure S2). According to previous reports,[24-27] the selective enhancement of this particular band in the SERS spectra of aromatic molecules is due to the presence of resonant metal-to-molecule CT processes (SERS-CT), which is the most important contribution to the chemical enhancement mechanism of SERS.

Several physicochemical factors (e.g., hapticity, ion/dipole/quadrupole, ion–π or π–π interactions) can be involved in building the supramolecular architecture of the interface. The interactions between PQ^{2+}, the anionic species, and the substrate are responsible for the complex electronic structure of the whole system in its ground and excited states and govern all the interfacial properties, including the corresponding SERS spectra. Electric potentials subtly modulate this electronic structure and specifically modulate the CT states, whose energies are strongly dependent on the applied potential.[26,28] Electrochemical SERS experiments were carried

ARTICLE

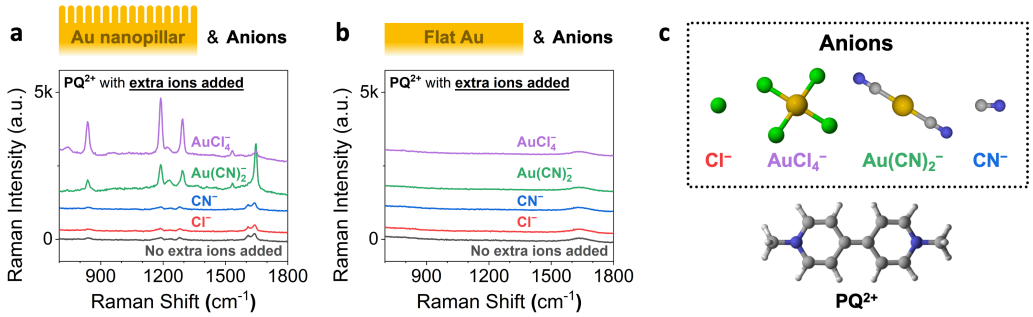

Figure 2. (a,b) SERS spectra from (a) Au nanopillar substrates and (b) flat Au substrates, recorded at the respective open-circuit potentials (OCPs) of a 5 μM PQ^{2+} aqueous solution (black, OCP: 0.32 V) and those recorded after anionic species were added to the original sample: Cl^- (1 mM, red, OCP: 0.32 V), CN^- (1 mM, blue, OCP: 0.35 V), $Au(CN)_2^-$ (1 mM, green, OCP: 0.24 V) and $AuCl_4^-$ (1 mM, purple, OCP: 0.80 V) (785 nm excitation). All solutions contained 0.1 M NaCl. (c) Structures of PQ^{2+} and of the anions selected as "molecular modulators."

out to confirm the CT-resonant origin of the (8a+8a') enhancement. Figures 3a and 3b show the dependence of the SERS spectra on the electrode potential E_V applied to Au nanopillar substrates in solutions containing $AuCl_4^-$ and $Au(CN)_2^-$, respectively. In both cases, the intensity of the (8a+8a') band is sensitive to the potential, reaching a maximum (V_{MAX}) in the spectra at +0.1 V in the case of $AuCl_4^-$ and −0.1 V in the case of $Au(CN)_2^-$. These spectra show an overall enhancement of the SERS effect as well as a selective intensification of the (8a+8a') mode when compared with the normal Raman spectrum (Figure 1a). These results imply that the energies of the CT excited states of the samples with $AuCl_4^-$ and $Au(CN)_2^-$ are in resonance with the 785 nm excitation line at the respective V_{MAX} potentials. When flat Au substrates were used, however, the influence of electrode potential was hardly caught (Figure 3e), which shows once again the key role of plasmons localized on the surface of nanostructured substrates. SERS spectra recorded at more negative potentials for samples with $AuCl_4^-$ were not included in Figure 3a because the dissolved oxygen was reduced and the spectra showed bands of decomposition products (see Figure S4 for details).

We can now explain the different enhancements of the (8a+8a') band in the SERS spectra of PQ^{2+} in the presence of $AuCl_4^-$ and $Au(CN)_2^-$ (Figure 2). These spectra were recorded at

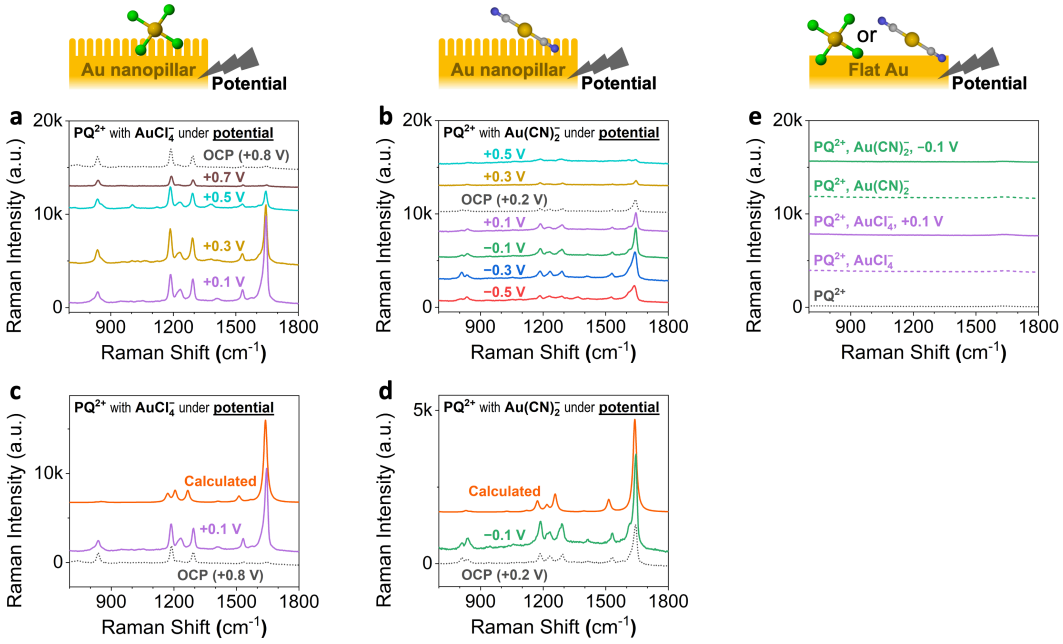

Figure 3. EC-SERS spectra measured from (a-d) Au nanopillar substrates and (e) flat Au substrates. SERS spectra (785 nm excitation) of 5 µM PQ^{2+} in 0.1 M NaCl aqueous solutions with (a) 1 mM $AuCl_4^-$ and (b) 1 mM $Au(CN)_2^-$, recorded at OCP and at different electric potentials. The SERS spectra theoretically calculated using TD-M06-HF/LanL2DZ (scaled wavenumbers ×0.93) for a system in resonance with the respective CT excited states are compared in figures (c) and (d) with the experimental SERS spectra of both samples recorded at the corresponding OCPs and V_{MAX} potentials. (e) SERS spectra of 5 µM PQ^{2+} in 0.1 M NaCl aqueous solutions with 1 mM $AuCl_4^-$ (purple) or 1 mM $Au(CN)_2^-$ (green), recorded at OCP (dashed) or V_{MAX} (solid, +0.1 V for $AuCl_4^-$ and −0.1 V for $Au(CN)_2^-$).

the respective OCPs (+0.80 and +0.24 V, respectively). The (8a+8a') band is very weak in the OCP spectrum with $AuCl_4^-$ given that the system is far from resonance (V_{MAX} = 0.1 V), whereas that with $Au(CN)_2^-$ should be in pre-resonance with the CT state (V_{MAX} = −0.1 V). The substantial difference between the respective OCP values reflects the differentiated surface charge of nanopillars, which is modulated by the nature of the added gold complex.[29] Au has different oxidation states in the $Au(III)Cl_4^-$ and $Au(I)(CN)_2^-$ complexes, being closely related to their respective standard reduction potentials of +0.79 V[30] and −0.8 V[31] (*vs* Ag/AgCl), respectively. That is, the adsorption of $AuCl_4^-$ or $Au(CN)_2^-$ molecular modulators modifies the electric properties of the bulk (potential) and the surface (excess of charge) of Au nanopillars differently. The combined electrical effect of the chemical adsorption and the applied potentials controls the energy of the CT processes (Figure S5) and explains the different behaviors observed in the respective SERS spectra.

We demonstrated the existence of metal-to-molecule CT states with energies likely to be excited under 785 nm excitation by carrying out electronic structure calculations following a previously reported methodology[7, 13-14, 27] based on time-dependent TD-M06-HF/LanL2DZ calculations (see details in the Supporting Information). Figure 4a shows the dependence of the calculated energies of the metal-to-molecule CT excited states (E_{CT}) on the density of charge (q_{eff}) of Au_n^q–$AuCl_4^-$–PQ^{2+} and Au_n^q–$Au(CN)_2^-$–PQ^{2+} supermolecules, respectively, where the anionic complexes and PQ^{2+} were bonded to a single terminal atom of the linear Au_n^q clusters (Figures 4b and S6).

Electrode potentials tune almost linearly the surface excess of charge of the electrode, which is simulated in the calculations through the mean density of charge ($q_{eff} = q/n$) of the stick-like Au_n^q clusters with different lengths (n) and charges (q). The values of q_{eff} range from +0.33 to −0.33 a.u. for the extreme cases of Au clusters containing three atoms with +1 or −1 a.u. charges (i.e., Au_3^{+1} to Au_3^{-1}), respectively (q_{eff} = −0.33 a.u. results are not discussed given that, in this case, two electrons of the Au_3^{-1} cluster are transferred to PQ^{2+} in their respective

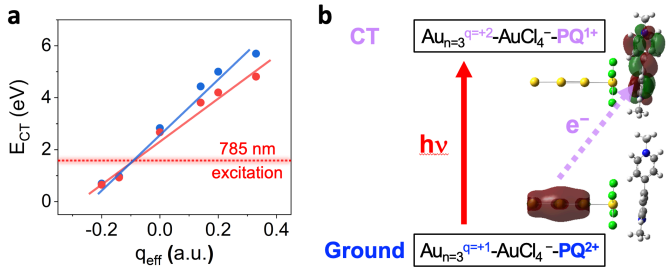

Figure 4. (a) Dependence of the TD-M06-HF/LanL2DZ calculated vertical energies of the metal-to-molecule CT excited states on the density of charge ($q_{eff} = q/n$) of Au_n^q–$AuCl_4^-$–PQ^{2+} (blue) and Au_n^q–$Au(CN)_2^-$–PQ^{2+} (red) supermolecules. (b) Example of the orbitals involved in the photo-induced CT excitation of a single electron from the HOMO of the Au_n^q clusters to the LUMO of paraquat in the $Au_{n=3}^{q=+1}$–$AuCl_4^-$–PQ^{2+} system.

ground electronic states, giving the corresponding doubly reduced Au_3^{+1}–$AuCl_4^-$–PQ^0 or Au_n^{+1}–$Au(CN)_2^-$–PQ^0 species). In the same way that E_V controls the energy of CT transitions, the calculated E_{CT} values for the systems with $AuCl_4^-$ and $Au(CN)_2^-$ depend linearly on q_{eff} and show similar trends. The resonant CT condition is fulfilled when the E_{CT} line crosses the energy of the used laser, which occurs at $q_{eff,785\ nm} \approx -0.1$ a.u. with both $AuCl_4^-$ and $Au(CN)_2^-$ complexes, as evident in Figure 4a. The photo-induced CT process would occur at the electrode potential (V_{MAX}) necessary to reach $q_{eff,785\ nm}$; an electron located at the HOMO of the metal (Au_n^q) would then be phototransferred to the LUMO of PQ^{2+} in the triads with either $AuCl_4^-$ or $Au(CN)_2^-$, giving the respective Au_n^{q+1}–$AuCl_4^-$–PQ^{1+} and Au_n^{q+1}–$Au(CN)_2^-$–PQ^{1+} excited CT species (Figure 4b). Therefore, from the perspective of paraquat, all the CT transitions of both series of data shown in Figure 4a are similar given that the same states of the adsorbate are involved: the ground electronic states of the dicationic (PQ^{2+}) and monocationic (PQ^{1+}) species, respectively, which differ exclusively in their E_{CT} values. This explain why all of the calculated Raman spectra in resonance with any CT state of Au_n^q–$AuCl_4^-$–PQ^{2+} or Au_n^q–$Au(CN)_2^-$–PQ^{2+} show the same relative intensities (Figure S7).

The resonance Raman spectra corresponding to CT states were calculated as described in the Supporting Information and are characterized by the selective enhancement of the (8a+8a') vibration, in agreement with the experimental spectra recorded at the respective V_{MAX}. For instance, the SERS-CT spectra calculated for Au_8^0–$AuCl_4^-$–PQ^{2+} and Au_8^0–$Au(CN)_2^-$–PQ^{2+} (q_{eff} = 0 a.u.) were selected for comparison with the experimental ones measured at the corresponding V_{MAX} and OCP potentials in Figures 3c and 3d, respectively.

Therefore, the combined analysis of experimental and calculated results leads to the deduction that the adsorption of different metal complexes generates different surface states of the triads, as verified by the respective OCP and SERS spectra. We concluded that the same voltage applied to the $Au(III)Cl_4^-$ or $Au(I)(CN)_2^-$ interfaces yields a different excess of charge of the substrate and, thus, different E_{CT} values. That is, the CT resonance would occur at the same effective density of charge $q_{eff,785\ nm}$ = −0.1 a.u. for both systems (Figure 4a) but at different

V_{MAX}, depending on the nature of the intercalated chemical modulator.

Supramolecular chemistry has proven useful in SERS, especially using macrocycles, which can bring weak adsorbates, such as hydrophobic or electron-deficient molecules, near the surface of metal nanoparticles.[32] $AuCl_4^-$ and $Au(CN)_2^-$ are responsible for this task in the SERS of paraquat. In addition to this passive role, the intercalation of these complexes must also reduce the effectiveness of nonradiative relaxation channels, which are responsible for quenching any photon emission from molecules directly bonded to nanoparticles, including Raman scattering/SERS, as Tian *et al*.[33] demonstrated for plasmonic nanoparticles coated with an ultrathin shell of silica or alumina. Counterintuitively, however, our results show that this chemical

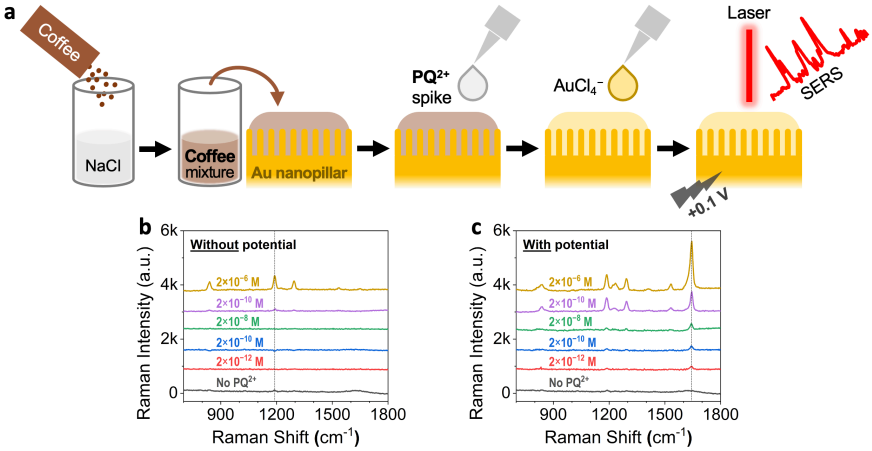

Figure 5. (a) Procedure for detecting PQ^{2+} in coffee samples using Au nanopillar substrates. (b,c) SERS spectra of PQ^{2+} in coffee at different PQ^{2+} concentrations in the presence of 1 mM $AuCl_4^-$ (b) without and (c) with the application of +0.1 V. Measurements were carried out without any pre-treatment procedure.

disconnection also favors the overall and selective enhancement observed in the SERS of PQ^{2+} given that an enhancement due to metal-to-molecule resonant CT processes has been observed. Intercalation should drastically reduce the overlap between donor and acceptor orbitals and, consequently, the probability of CT between them. We propose that the long-range electron transfer between the chemically disconnected Au substrate and paraquat occurs via a through-bond mechanism similar to the superexchange electron transfer model in donor–bridge–acceptor triads,[34] where $AuCl_4^-$ and $Au(CN)_2^-$ would play the role of the bridge. Superexchange transfer requires an intermediate virtual orbital of the bridge with an energy similar to those of the donor and the acceptor. This condition appears to be preserved in Au_n^q–$AuCl_4^-$–PQ^{2+} systems given that TD-M06-HF/LanL2DZ calculated energies of the metal-to-$AuCl_4^-$ (donor-to-bridge) and metal-to-PQ^{2+} (donor-to-acceptor) sets of CT states have similar trends. This requirement is fulfilled around q_{eff} = −0.1 a.u. under 785 nm excitation, as evident in Figure S8. However, the intermediate metal-to-bridge CT states are missing in the cases of Cl^- and CN^-, which accounts for the weaker enhancement of mode (8a+8a') in their SERS spectra.

Conceivably, the stronger SERS intensities recorded in $AuCl_4^-$ containing samples may have arisen from changes in the morphology of the nanopillar substrate given that new Au nanoparticles could be formed by electrochemical reduction of $AuCl_4^-$ at particular potentials to further enhance the electromagnetic field. However, this hypothesis was discarded because the SERS intensities after electrochemical treatment were weaker than those in the spectra recorded before the treatment (Figure S9).

Thus far, we have shown that anionic metal complexes can serve as effective chemical modulators for SERS enhancement but also that their resultant effects are dependent on the particular chemical nature of the involved systems. The dual modulation of the SERS intensities with anionic complexes and electric potentials is also observed in the spectra of other electron-deficient cationic molecules such as diquat (DQ^{2+}) and brilliant green, demonstrating the generality of this effect (Figure S10).

The practical application of this novel approach was evaluated for the on-site detection of pollutants in real samples. The technique was used to detect PQ^{2+} in coffee drink samples (spiked with PQ^{2+}) because coffee is one of the common crops on which PQ^{2+} herbicide is used (Figure 5a). No significant bands were observed in the SERS spectra of coffee drink samples recorded on Au nanopillar substrates. When $AuCl_4^-$ (1 mM) was added, the characteristic peaks of PQ^{2+} appeared and a limit of detection (LOD) of 2×10^{-6} M was obtained (Figure 5b). This concentration is greater than the maximum residue limit (MRL) for PQ^{2+} in coffee, as established by the European Union Commission (0.05 mg/kg; 1.9×10^{-7} M). The sensitivity was effectively improved below the MRL by applying a +0.1 V voltage (Figure 5c), resulting in an LOD as low as 2×10^{-12} M. This method also allows for the selective detection of PQ^{2+} in presence of related molecules; EC-SERS spectra of PQ^{2+}, another herbicide DQ^{2+}, and their mixture were measured, and it was found that the fingerprint bands of PQ^{2+} can be used to detect PQ^{2+} sensitively and selectively in the mixture (see details in Figure S11). These results demonstrate the usefulness of combining chemical and electrical modulators for rapid on-site ultrasensitive detection of hazardous substances.

Conclusions

In summary, we proposed a novel approach to further amplifying SERS signals by tuning CT resonance processes via supramolecular interactions and applied potentials. Both factors modulate the overall electronic structure of the interface, control the surface excess of charge of the metal, and tune the energy of electron transfer transitions. As a demonstration, the PQ^{2+} SERS signal was substantially amplified in the presence of Au-complex anions and further amplification was attained under applied potentials. The results of this study suggest a novel avenue for exploring the combined use of supramolecular interactions and electrode potentials for deep understanding of the structure and properties of electrified interfaces as well as for developing ultrasensitive SERS platforms.

Experimental

Materials

Paraquat dichloride, $PQCl_2$ (PQ^{2+}), gold(III) chloride trihydrate ($HAuCl_4{\cdot}3H_2O$), potassium dicyanoaurate ($K[Au(CN)_2]$), potassium cyanide (KCN), potassium phosphate monobasic (KH_2PO_4), and potassium phosphate dibasic trihydrate ($K_2HPO_4{\cdot}3H_2O$) were purchased from Sigma-Aldrich (St. Louis, MO, USA). Sodium chloride (NaCl) was purchased from Samchun (Pyeongtaek, South Korea). Deionized water (DIW, >18 MΩ·cm) was obtained from Human UP (Human Corp.). pH indicator solution was purchased from EMD Millipore Corp. (Darmstadt, Germany). All chemicals were dissolved in DIW. Phosphate buffer solution (0.1 M, pH 7.18) was prepared using KH_2PO_4 and $K_2HPO_4{\cdot}3H_2O$ solutions.

Fabrication and characterization of Au SERS substrates

Au SERS substrates were fabricated by depositing Au onto 250 µm-thick polyethylene terephthalate (PET) substrates. The PET substrates were treated with Ar plasma (power: 100 W, Ar flow rate: 30 sccm, chamber pressure: 32 mTorr, duration: 1 min) using a 13.56 MHz radio-frequency ion-etching instrument, resulting in polymeric nanopillars on the substrate. An Au film was deposited onto the Ar-plasma-treated nanopillars (power: 100 W, Ar flow rate: 20 sccm, chamber pressure: 7 mTorr, deposition rate: 2 Å/s) to a thickness of 100 nm using a sputtering system. The morphologies of the Au SERS substrates were characterized by field-emission scanning electron microscopy (FE-SEM; Joel JSM-6700F). The reproducibility of the morphologies was verified by the reproducible SERS signals from 12 different Au SERS substrates (see Figure S12),-measured with the same solution (5 µM PQ^{2+} in the presence of 1 mM $AuCl_4^-$) under the same experimental conditions (application of +0.1 V). The substrates were highly stable due to the chemical inertness of Au in air. Once a batch of substrates were fabricated, they provided a reproducible signal over, at least, a few months.

EC-SERS instrumentation and measurement

The electrochemical measurements were carried out using a potentiostat (ZIVE SP2, Wonatech) and a homemade electrochemical cell that held the Au working electrode, a Ag/AgCl (3 M NaCl) reference electrode, and a platinum (Pt) counter electrode. All electrode potentials were reported *vs* Ag/AgCl (3 M NaCl). The cell had a 0.07 cm^2 perforation in its center, which exposed the Au electrode to the analyte solution. The cell contained a total solution volume of 400 µL. Raman measurements were conducted *in situ* with an Ocean Optics portable probe spectrometer system (UQEPRO-Raman) equipped with a 785 nm laser source. The laser power was 30 mW, and the integration time was 1 s.

For the EC-SERS measurements, the Au electrode surface was first electrochemically cleaned using cyclic voltammetry (CV). The potential was scanned between 0 and 1.1 V at a scan rate of 0.05 V/s in 400 µL phosphate buffer solution as the current was measured. The phosphate buffer solution was changed after the cycling, and the measurement was repeated until a reproducible cyclic voltammogram was obtained.

After the Au electrode surface was cleaned and rinsed, 392 µL of NaCl solution was added to the cell. A 4 µL aliquot of paraquat (PQ^{2+}, 500 µM dissolved in DIW) was first added to the NaCl solution, and PQ^{2+} Raman spectra were acquired for a period of time. Afterwards, 4 µL of $HAuCl_4$ (100 mM dissolved in DIW) was added to the solution. The final concentrations of PQ^{2+} and $AuCl_4^-$ were 5 µM and 1 mM, respectively (unless stated otherwise). After careful mixing, the solution was allowed to stabilize under irradiation by the laser before real-time data acquisition began. Raman spectra were collected for 30 s, after which a constant potential was applied to the electrode for 60 s (unless otherwise stated). Maximum signal enhancement was attained 4 s from the onset of the applied potential; however, spectra were acquired for the entire potential application period. Spectra were acquired continuously for 30 s after the potential was terminated.

Paraquat detection in coffee

The coffee drink was prepared according to the recommended serving (0.9 g/120 mL) and diluted 1000-fold in 0.1 M NaCl. The intrinsic Raman responses of coffee in $AuCl_4^-$ with and without the applied potential were obtained and used as a baseline for spectral background subtraction. Measurements were carried out without treatment of the coffee powder and coffee solution samples.

Author Contributions

Iris B. Ansah: Formal Analysis, Investigation, Methodology, Writing – original draft. **Daniel Aranda**: Formal analysis, Investigation, Writing – original draft. **Ho S. Jung**: Writing – review & editing. **Sung-Gyu Park**: Resources, Writing – review & editing. **Mijeong Kang**: Conceptualization, Investigation, Methodology, Writing – original draft. **Juan C. Otero**: Conceptualization, Funding acquisition, Investigation, Methodology, Writing – original draft. **Dong-Ho Kim**: Conceptualization, Funding acquisition, Investigation, Methodology, Supervision, Writing – original draft

Conflicts of interest

There are no conflicts to declare.

Acknowledgements

This project was supported by the Fundamental Research Program (PNK 7440) of the Korea Institute of Materials Science (KIMS), by the National Research Foundation of Korea (NRF) grant funded by the Korean government (MSIT) (NRF-2021R1C1C1010213), and by Junta de Andalucía/FEDER (UMA18-FEDERJA-049 and P18-RT-4592). DA thanks the Fundacion Ramon Areces (Madrid) for postdoctoral grant.

Notes and references

1 Langer, J, Jimenez de Aberasturi, D, Aizpurua, J, Alvarez-Puebla, R. A, Auguié, B, Baumberg, J. J, Bazan, G. C, Bell, S. E. J, Boisen, A, Brolo, A. G, Choo, J, Cialla-May, D, Deckert, V, Fabris, L, Faulds, K, García de Abajo, F. J, Goodacre, R, Graham, D, Haes, A. J, Haynes, C. L, Huck, C, Itoh, T, Käll, M, Kneipp, J, Kotov, N. A, Kuang, H, Le Ru, E. C, Lee, H. K, Li, J.-F, Ling, X. Y, Maier, S. A, Mayerhöfer, T, Moskovits, M, Murakoshi, K, Nam, J.-M, Nie, S, Ozaki, Y, Pastoriza-Santos, I, Perez-Juste, J, Popp, J, Pucci, A, Reich, S, Ren, B, Schatz, G. C, Shegai, T, Schlücker, S, Tay, L.-L, Thomas, K. G, Tian, Z.-Q, Van Duyne, R. P, Vo-Dinh, T, Wang, Y, Willets, K. A, Xu, C, Xu, H, Xu, Y, Yamamoto, Y. S, Zhao, B, Liz-Marzán, L. M., *ACS Nano* 2020, **14**, 28-117.

2 Ding, S.-Y, You, E.-M, Tian, Z.-Q, Moskovits, M., *Chem. Soc. Rev.* 2017, **46**, 4042-4076.

3 Park, S.-G, Mun, C, Xiao, X, Braun, A, Kim, S, Giannini, V, Maier, S. A, Kim, D.-H., *Adv. Funct. Mater.* 2017, **27**, 1703376.

4 Pilot, R, Signorini, R, Durante, C, Orian, L, Bhamidipati, M, Fabris, L., *Biosensors* 2019, **9**, 57.

5 Campion, A, Kambhampati, P., *Chem. Soc. Rev.* 1998, **27**, 241-250.

6 Wu, D.-Y, Liu, X.-M, Duan, S, Xu, X, Ren, B, Lin, S.-H, Tian, Z.-Q., *J. Phys. Chem. C* 2008, **112**, 4195-4204.

7 Aranda, D, Valdivia, S, Avila, F. J, Soto, J, Otero, J. C, López-Tocón, I., *Phys. Chem. Chem. Phys.* 2018, **20**, 29430-29439.

8 Selvakannan, P. R, Ramanathan, R, Plowman, B. J, Sabri, Y. M, Daima, H. K, O'Mullane, A. P, Bansal, V, Bhargava, S. K., *Phys. Chem. Chem. Phys.* 2013, **15**, 12920-12929.

9 Wu, D.-Y, Li, J.-F, Ren, B, Tian, Z.-Q., *Chem. Soc. Rev.* 2008, **37**, 1025-1041.

10 Gieseking, R. L, Ratner, M. A, Schatz, G. C., *Faraday Discuss.* 2017, **205**, 149-171.

11 Aranda, D, Valdivia, S, Soto, J, López-Tocón, I, Avila, F, Otero, J. C., *Front. Chem.* 2019, ***7***, 423.

12 Aranda, D, Román-Pérez, J, López-Tocón, I, Soto, J, Ferrer, F. J, Otero, J. C., *Phys. Chem. Chem. Phys.* 2017, **19**, 27888-27891.

13 Valdivia, S, Aranda, D, Ferrer, F. J. A, Soto, J, López-Tocón, I, Otero, J. C., *J. Phys. Chem. C* 2020, **124**, 17632-17639.

14 Avila, F, Fernandez, D. J, Arenas, J. F, Otero, J. C, Soto, J., *Chem. Commun.* 2011, **47**, 4210-4212.

15 Zhu, Y, Wu, J, Gao, H, Liu, G, Tian, Z, Feng, J, Guo, L, Xie, J., *RSC Adv.* 2016, **6**, 59919-59926.

16 Giese, M, Albrecht, M, Rissanen, K., *Chem. Commun.* 2016, **52**, 1778-1795.

17 Schottel, B. L, Chifotides, H. T, Dunbar, K. R., *Chem. Soc. Rev.* 2008, **37**, 68-83.

18 Wang, D.-X, Wang, M.-X., *J. Am. Chem. Soc.* 2013, **135**, 892-897.

19 Kim, D, Tarakeshwar, P, Kim, K. S., *J. Phys. Chem. A* 2004, **108**, 1250-1258.

20 Bauzá, A, Mooibroek, T. J, Frontera, A., *CrystEngComm* 2016, **18**, 10-23.

21 Caracelli, I, Zukerman-Schpector, J, Tiekink, E. R. T., *Gold Bull.* 2013, **46**, 81-89.

22 Chen, Y, Wang, F., *J. Mol. Model.* 2015, **21**, 38.

23 Tiekink, E. R. T, Zukerman-Schpector, J., *CrystEngComm* 2009, **11**, 2701-2711.

24 Centeno, S. P, López-Tocón, I, Roman-Perez, J, Arenas, J. F, Soto, J, Otero, J. C., *J. Phys. Chem. C* 2012, **116**, 23639-23645.

25 Liu, L, Chen, D, Ma, H, Liang, W., *J. Phys. Chem. C* 2015, **119**, 27609-27619.

26 Avila, F, Ruano, C, Lopez-Tocon, I, Arenas, J. F, Soto, J, Otero, J. C., *Chem. Commun.* 2011, **47**, 4213-4215.

27 Román-Pérez, J, López-Tocón, I, Castro, J. L, Arenas, J. F, Soto, J, Otero, J. C., *Phys. Chem. Chem. Phys.* 2015, **17**, 2326-2329.

28 Roman-Perez, J, Ruano, C, Centeno, S. P, López-Tocón, I, Arenas, J. F, Soto, J, Otero, J. C., *J. Phys. Chem. C* 2014, **118**, 2718-2725.

29 Anderson, S. R, Mohammadtaheri, M, Kumar, D, O'Mullane, A. P, Field, M. R, Ramanathan, R, Bansal, V., Robust *Adv. Mater. Interfaces* 2016, **3**, 1500632.

30 Au, L, Lu, X. M, Xia, Y. N., *Adv. Mater.* 2008, **20**, 2517-2517.

31 Henglein, A, Meisel, D., *Langmuir* 1998, **14**, 7392-7396.

32 Montes-García, V, Fernández-López, C, Gómez, B, Pérez-Juste, I, García-Río, L, Liz-Marzán, L. M, Pérez-Juste, J, Pastoriza-Santos, I., *Chem. Eur. J*. 2014, **20**, 8404-8409.

33 Li, J. F, Huang, Y. F, Ding, Y, Yang, Z. L, Li, S. B, Zhou, X. S, Fan, F. R, Zhang, W, Zhou, Z. Y, Wu, D. Y, Ren, B, Wang, Z. L, Tian, Z. Q., *Nature* 2010, **464**, 392-395.

34 Benniston, A. C, Harriman, A., *Chem. Soc. Rev.* 2006, **35**, 169-179.